Journal of Fluorescence (2023) 33:437–444
https://doi.org/10.1007/s10895-022-03096-w

RESEARCH

# Synthesis and Photophysical Study of Tetraphenyl Substituted BODIPY Based Phenyl-Monoselenide Probe for Selective Detection of Superoxide

**Shrikrishna T. Salunke[1,2] · Divyesh S. Shelar[1] · Sudesh T. Manjare[1]**

Received: 12 October 2022 / Accepted: 18 November 2022 / Published online: 26 November 2022


**Abstract**
Selenium containing tetraphenyl substituted BODIPY probe was successfully synthesized from respective selenium aldehyde and tetraphenyl pyrrole using Knoevenagel-type condensation. The product was characterized using various spectroscopic techniques ($^{1}$ H, $^{13}$ C, $^{77}$Se, $^{11}$B, and $^{19}$ F) and mass spectrometry. The probe was found to be selective and sensitive towards detection of superoxide over other ROS with a "*turn-off*" (quenched) fluorescence response. The detection limit of the probe was found to be 4.87 µM. The probe reacted with superoxide in less than a sec with a stoke shift of 35 nm.

**Keywords** BODIPY · Organoselenium · Superoxide · Sensor · Reactive oxygen species

## Introduction

In recent decades organoselenium compounds have been investigated as fluorophores due to the hard/soft characteristic of selenium, which enables it to detect certain analytes. In the biological system, bioactive chemicals such as thiols, reactive oxygen species (ROS), reactive nitrogen species (RNS), and others play a vital role [1–6]. Alzheimer's disease (AD) is the most common type of dementia among older people [7–10]. A related problem, mild cognitive impairment (MCI) causes more memory problems than normal for people of the same age but not all, people with MCI will develop AD. According to recent studies, the disease is supposed to be based on three main hypotheses namely Amyloidal cascade, Metal ions, and Reactive Oxygen Species [10, 11]. As metal ions and ROS are among the causes of this disease it is very important to detect them selectively.

BODIPY and its derivatives constitute an important class of compounds in heterocyclic organic chemistry [12, 13]. Recent development in the field of modern science and medicine such as material science, molecular biology, light-harvesting systems, analytical and environmental chemistry emphasizes the use of BODIPY fluorophore [14]. BODIPY (i.e., 4,4-difluoro-4-bora-3a,4a-diaza-5-indacene) derivatives are strongly UV absorbing small molecular probes having good photophysical characteristics like high quantum yields, high thermal and chemical stabilities [15–17]. Despite of wide applicability, the synthetic access to near IR BODIPY dyes is neither facile nor efficient. Many attempts to develop NIR probes have been made [18]. However, still, there is a lot of scope for the new development of NIR probes.

Recently some chalcogen containing small molecular probes have attracted the focus of researchers [19]. Main challenge for the organochalcogen chemist is to synthesize a novel heterocyclic system. In recent past biologically active selenium based chalcogen compounds have been discovered and used for redox reactions [20–22]. However, there is very little development on chalcogen-containing compounds as sensors, antioxidant, anti-inflammatory, neoplastic, and antifungal capabilities [23–26].

Researchers have shown more interest in synthesis and application of organoselenium compounds for the selective discovery of physiologically significant analytes in recent years [27–30]. A variety of fluorophores have been developed for better understanding of superoxide, including

✉ Sudesh T. Manjare
sudeshmanjare@chemistry.mu.ac.in

[1] Department of Chemistry, University of Mumbai, Vidyanagari, 400098 Mumbai, India

[2] Department of Chemistry, T.C. College, 413102 Baramati, India

fluorescein, dibenzothiazoline cyclohexene, and BODIPY [31, 32]. There have been some reports on the use of a phenyl cellulose-modified probe to detect ROS selectively and in real-time [33]. The electronic environment around the selenium in the probe changes as ROS reacts. This allows the spectrophotometric changes in the probe, such as fluorescence "*turn-on*" and "*turn-off*" events, which assist in the fluorescence detection of the analyte [34–38].

Currently we have focused on the development of a new organochalcogen embedded BODIPY derivatives, as well as the synthetic modification and spectroscopic characterization of this bright small-molecule. Here in this work we have developed near-IR selenium containing tetraphenyl substituted BODIPY (Se-BODIPY) probe for selective detection of superoxide.

## Experimental

### Materials and Methods

All the required chemicals (analytical grade) were obtained from commercial dealers and used without being purified. All the solvents utilized in the spectrum evaluation were of analytical grade or HPLC grade. O–formyl–phenyl selenide and 2,4-diphenyl pyrrole were synthesized by using known literature procedure [39, 40]. The silica gel (60–120) was used for column chromatography. With Bruker Avance 300 and 600 MHz instruments the $^{1}$H, $^{13}$C, $^{11}$B, $^{19}$F and $^{77}$Se NMR spectra were recorded. For $^{1}$H and $^{13}$C NMR spectroscopy, tetramethyl silane (TMS) was used as internal standard, while $Ph_2Se_2$ was used as an external standard for $^{77}$Se NMR spectroscopy. The NMR spectrum of all the compounds were recorded in analytical and HPLC grade deuterated solvents. The mass spectra were recorded on AB SCIEX 3200 Q TRAP LC/MS/MS spectrometer. Shimadzu UV2450 PC spectrometer was used to record UV spectra. Shimadzu RF 5301PC Spectrofluorometer was used to obtain emission spectra. MicroTOF–QII was used to collect HRMS data (Bruker Daltonik).

### Synthesis of BODIPY (3)

The Bodipy was synthesized from a reported procedure with some modifications [41]. 2-phenylselenyl benzaldehyde (0.5 g, 1.90 mmol, 1 eqv.) and 2,4-diphenyl pyrrole (0.91 g, 4.19 mmol, 2.2 eqv.) were dissolved in dry DCM (25 mL), a catalytic amount of TFA was added and the reaction mixture was stirred overnight at room temperature under a nitrogen atmosphere. After complete consumption of reactants, 2,3-dichloro-5,6-dicynobenzoquinone (0.86 g, 3.816 mmol, 2 eqv.) was added and the reaction mixture was stirred for 1 h at room temperature. After 1 h, triethylamine (3.85 g, 38.167 mmol, 20 eqv.) was added and stirred the reaction for 15 min, then $BF_3.Et_2O$ (5.41 g, 38.167 mmol, 20 eqv.) was added. Stirring of the mixture was continued for an additional 3 h at room temperature. The progress of the reaction was followed by TLC. The reaction was quenched with water and extracted with dichloromethane (3 × 25 mL). The combined organic layer was dried over $Na_2SO_4$ and the solvent was removed in vacuum under reduced pressure. The crude product was purified by silica-gel column chromatography, eluting with an ethyl acetate-hexane (1:3). Dark purple colour solid product (**3**) was obtained in the yield of 0.31 g (22%). The targeted BODIPY (**3**) was confirmed by $^{1}$H, $^{13}$C, $^{77}$Se, $^{11}$B, $^{19}$F NMR spectroscopy, as well as HR-LCMS. Spectroscopic Data:- $^{1}$H NMR (600 MHz, $CDCl_3$) δ ppm: 7.93–7.92 (dd, J = 8.0, 1.4 Hz, 4 H), 7.57–7.55 (dd, J = 8.0, 1.4 Hz, 2 H), 7.43–7.41 (m, 6 H), 7.36–7.34 (m, 3 H), 6.96–6.95 (d, J = 7.1 Hz, 4 H), 6.89–6.84 (m, 6 H), 6.79–6.77 (dd, J = 7.3, 1.6 Hz, 1 H), 6.50 (s, 2 H), 6.38–6.35 (m, 2 H), 6.11–6.10 (dd, J = 7.7, 1.1 Hz, 1 H); $^{13}$C NMR (151 MHz, $CDCl_3$) δ ppm: 156.4, 146.7, 142.6, 135.6, 135.3, 134.1, 131.7, 131.6, 131.3, 130.3, 128.6, 128.5, 128.5, 128.4, 127.9, 127.7, 127.1, 126.9, 126.6, 125.7, 125.5, 123.2, 122.6, 76.3, 76.2, 76.0, 76.0, 75.8; $^{77}$Se NMR (114 MHz, $CDCl_3$) δ ppm: 421; $^{11}$B NMR (193 MHz, $CDCl_3$) δ ppm: 0.45; $^{19}$F NMR (565 MHz, $CDCl_3$) δ ppm: -130.02 (ddd), -133.22 (m); ESI-MS calculated for $(C_{45}H_{31}BF_2N_2Se + Na)^+$: 751.52, found m/z 751.16 $(M + Na)^+$.

### Synthesis of Oxidized Probe (4)

Probe **3** (0.10 g, 0.137 mmol) was dissolved in DMSO-$d_6$ (0.6 mL) and $KO_2$ (0.097 g, 1.37 mmol, 10 eqv.) was dissolved in 0.5 mL DMSO-$d_6$. The reaction mixture was stirred at room temperature for 30 min. The progress of the reaction was monitored by TLC. The oxidized probe (**4**) was characterized without isolation and confirmed by $^{1}$H NMR spectroscopy, and mass spectrometry. Spectroscopic Data;- $^{1}$H NMR (300 MHz, DMSO-$d_6$) δ ppm: 8.01-8.0 (d, J = 3.6 Hz, 1 H), 7.83–7.82 (d, J = 3.6 Hz, 2 H), 7.67–7.65 (d, J = 4.9 Hz, 4 H), 7.55–7.54 (d, J = 4.1 Hz, 2 H), 7.34–7.32 (d, J = 4.5 Hz, 3 H), 7.20–7.19 (d, J = 3.4 Hz, 8 H), 7.09–7.08 (d, J = 4.5 Hz, 4 H), 6.80–6.78 (m, 3 H), 6.66 (s, 1 H), 6.33 (s, 1 H), 5.89–5.86 (m, 2 H). ESI-MS calculated for $(C_{45}H_{31}BF_2N_2SeO)^+$: 743.52, found m/z 743.5 $(M)^+$.

### Photophysical Measurements

All photophysical study was conducted in DMSO. ROS ($H_2O_2$, NaOCl, $^{t}$BuOOH, $^{\bullet}$OH, and $^{t}$BuO$^{\bullet}$; 0.1 M) and biothiols (glutathione, L–cysteine, D–L–homocysteine,

**Scheme 1** Synthesis of Compound **3**

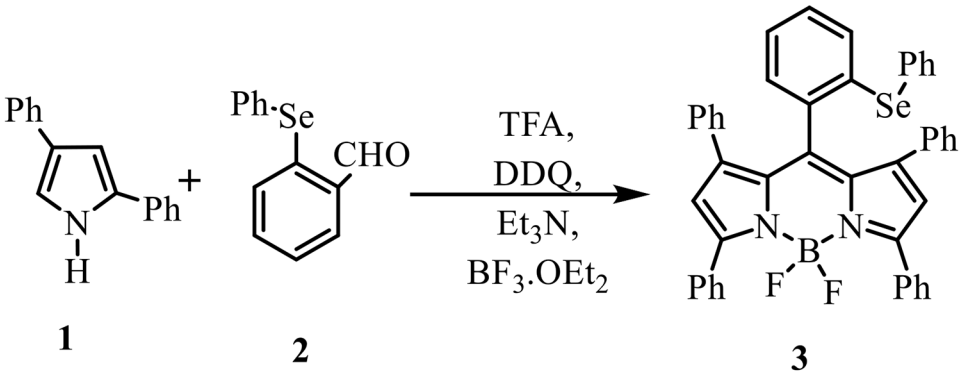


N–acetyl–L–cysteine, and D-methionine; 0.1 M) were prepared in double distilled water, whereas $KO_2$ (0.1 M), was prepared in DMSO. Before absorbance and fluorescence measurements, the probe (5 μM) was incubated for 2 min with ROS and biothiols at rt. All solutions were excited at a wavelength of $\lambda_{ex} = 573$ nm and emission was recorded at $\lambda_{em} = 608$ nm, excitation and emission slit width was taken 5/5 nm respectively.

### Selectivity and Sensitivity of the Probe in the Presence of ROS

The probe (**3**) was screened with ROS ($KO_2$, $H_2O_2$, $^t$BuOOH, NaOCl, $^{\bullet}$OH, and $^t$BuO$^{\bullet}$; 800 μM) and biothiols (glutathione, L–cysteine, D–L–homocysteine, N–acetyl–L–cysteine, and D-methionine; 800 μM). After 2 min of the incubation period, UV-Vis and fluorescence spectra were taken.

### Interference Study

Probe (**3**) (3 mL, 5 μM) and superoxide (24 μL, 800 μM) were introduced to each vials followed by other ROS and biothiols of 24 μL (800 μM) each. After 2 min of incubation, fluorescence was recorded at an excitation wavelength of $\lambda_{ex} = 573$ nm.

### Detection Limit

An increase in concentration measurements were carried out to determine detection limit. 3 mL (5 μM) of the probe (**3**) in the presence of increasing concentrations of superoxide (0-800 μM; 0–24 μL) was incubated for 2 min and fluorescence spectra were recorded at 573 nm. The limit of detection was calculated by fluorescence linear regression curve. The standard deviation of the probe was determined by recording emission of probe **3** for ten times at 573 nm. The fluorescence intensity at 608 nm was plotted against the concentration of superoxide to evaluate the slope. The detection limit was calculated by using equation.

$LOD = 3\sigma/k$.

Where, σ is standard deviation of the probe and k is the slope of plot of fluorescence intensity vs. concentration of superoxide.

### Time-dependent Study

The time-dependent emission study was performed with probe **3** (3 mL, 5 μM) in the presence of superoxide (24 μL, 800 μM) for a period of 1 h. The excitation and emission wavelength for this kinetic experiment was 573 and 608 nm, excitation and emission slit width was 5/5 nm respectively.

## Results and Discussion

### Design and Synthesis of Probe 3

2,4-diphenyl pyrrole was synthesized from the chalcone (1,3-diphenyl-2-propen-1-one) by the aldol condensation reaction of acetophenone with benzaldehyde in the presence of sodium hydroxide (Scheme 1) [42]. Chalcone was converted into its nitro derivative (1,3-diphenyl-4-nitrobutane-1-one) by using a Michael addition process using nitromethane and diethylamine as a base [43]. 2,4-diphenylpyrrole (**1**) was synthesized according to literature by reacting nitro-chalcone with morpholine, sulphur, and ammonium acetate [39]. 2-phenylselenyl benzaldehyde (**2**) was synthesized using reported literature method, where 2-chlorobenzaldehyde was reacted with diphenyl diselenide in presence of DTT and $K_2CO_3$ in DMF [40]. Compound **2** was confirmed by the $^1$H NMR spectroscopy before further use.

Then 2-phenylselenyl benzaldehyde **2** was converted into the corresponding dipyrromethane by reaction with 2,4-diphenyl pyrrole in presence of the catalytic amount of trifluoroacetic acid (TFA). The in situ formed

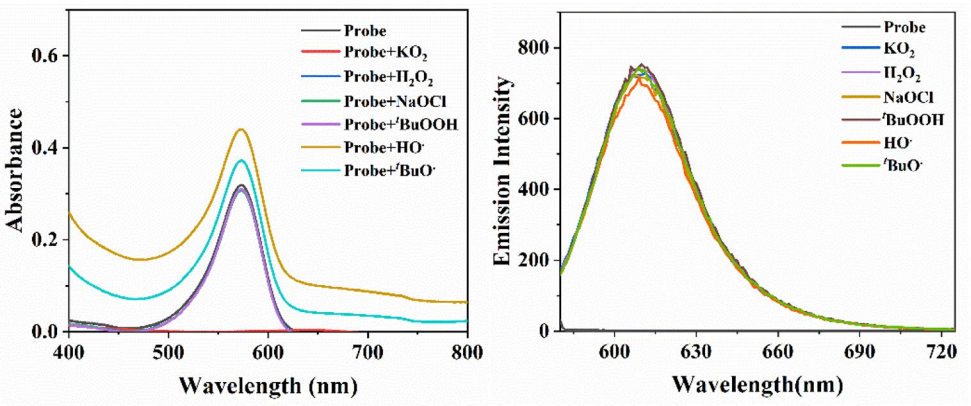


**Fig. 1** (Left) UV–absorption spectra of probe **3** (5 µM) in DMSO with ROS (800 µM) ($KO_2$, $H_2O_2$, NaOCl, $^t$BuOOH, $^{\bullet}$OH and $^t$BuO$^{\bullet}$) incubated for 2 min at rt. (Right) Emission spectra of probe **3** (5 µM) in DMSO with ROS (800 µM) ($KO_2$, $H_2O_2$, NaOCl, $^t$BuOOH, $^{\bullet}$OH and $^t$BuO$^{\bullet}$) incubated for 2 min at rt ($\lambda_{ex}$ = 573 nm, $\lambda_{em}$ = 608 nm), slit width 5/5 nm

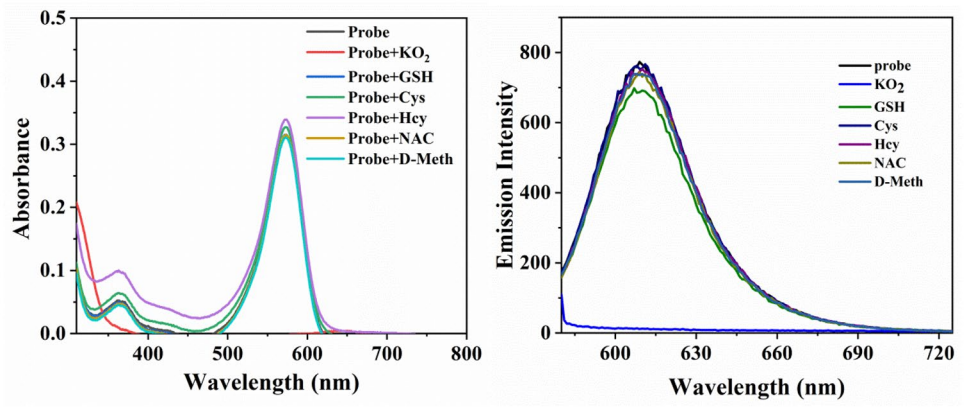


**Fig. 2** (Left) UV–absorption spectra of biothiols (800 µM) (GSH, Cys, Hcy, NAC, D-Meth) with probe **3** (5 µM) in DMSO incubated for 2 min at rt. (Right) Emission spectra of probe **3** (5 µM) in DMSO with biothiols (800 µM) (GSH, Cys, Hcy, NAC, D-Meth) incubated for 2 min at rt ($\lambda_{ex}$ = 573 nm, $\lambda_{em}$ = 608 nm), slit width 5/5 nm

dipyrromethane was then treated with 2,3-dichloro-5,6-dicynobenzoquinone (DDQ) followed by triethylamine and boron trifluoride ethyletharate in dry DCM. The reaction was monitored by TLC and the crude product was purified by column chromatography (yield 22%). The product was characterized by common spectroscopic techniques ($^1$ H, $^{13}$ C, $^{11}$B, $^{19}$ F and $^{77}$Se NMR) and mass spectrometry (Figs. S1-9).

The $^1$ H NMR spectrum of probe **3** showed a singlet at 6.50 ppm for proton attached to pyrrole ring carbon (HC = C-) (Fig. S1). The $^{77}$Se NMR signal of probe **3** was observed at 421 ppm (Fig. S4). The HR-LCMS of the probe (**3**) showed a $(C_{45}H_{31}BF_2N_2Se + Na)^+$ ion peak at 751.16 with a selenium isotopic pattern (Fig. S9). Thus, the spectroscopic analysis confirmed the successful formation of probe **3**.

## Photophysical Studies of Probe 3

Selenium-containing probe **3** was prepared to detect the responses arising from the oxidation of selenium by ROS. The probe was incubated with different ROS and biothiols for 2 min before recording absorption and emission spectra. In UV-visible study, the probe (**3**) and the probe with other ROS ($H_2O_2$, NaOCl, $^t$BuOOH, $^{\bullet}$OH and $^t$BuO$^{\bullet}$) and biothiols (GSH, Cys, Hcy, NAC, D-Meth) showed maximum absorbance at 573 nm whereas probe **3** with superoxide did not show any absorbance in the UV-visible spectrum (Figs. 1 and 2). The emission spectra revealed the quenching in fluorescence of probe **3** after reacting with superoxide (Fig. 1, S12-13). However, probe **3** and the probe with other ROS showed the emission peak at 608 nm. Similarly, the probe **3** with biothiols exhibited the emission peak at 608 nm. Thus, these results suggested the selectivity of the probe for superoxide over other ROS and biothiols with *turn-off* fluorescence.

Next, the interference study of the probe with superoxide in presence of other ROS was performed. Probe **3** (3 mL, 5 µM) and superoxide (800 µM) were added to each vial, followed by other reactive oxygen species such as $H_2O_2$, NaOCl, $^t$BuOOH, $^{\bullet}$OH, and $^t$BuO$^{\bullet}$ (800 µM) (Fig. 3) and fluorescence was recorded. From the study it was observed that there was no effect of the other ROS on the fluorescence intensity of the probe with superoxide.

An increase in the concentration study was performed with probe **3** (5 µM) in presence of superoxide (0-800 µM) to reveal the detection limit of the probe (Fig. 4). With increasing concentration of superoxide (0-800 µM), a steady decrease in fluorescence intensity of the probe (**3**) was observed. The detection limit was deduced using

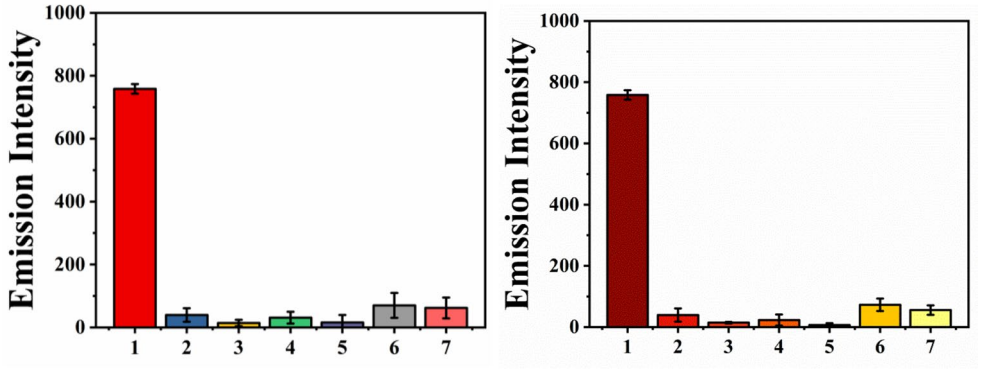


**Fig. 3** Fluorescence spectra of probe **3** (5 µM) and superoxide (800 µM) in presence of (Left) ROS ($H_2O_2$, NaOCl, $^t$BuOOH, $^{\bullet}$OH and $^t$BuO$^{\bullet}$) (800 µM) (1 = probe, 2 = probe + $KO_2$, 3 = probe + $KO_2$ + $H_2O_2$, 4 = probe + $KO_2$ + NaOCl, 5 = probe + $KO_2$ + $^t$BuOOH, 6 = probe + $KO_2$ + $^{\bullet}$OH, 7 = probe + $KO_2$ + $^t$BuO$^{\bullet}$); (Right) Biothiols (GSH, Cys, Hcy, NAC, D-Meth) (800 µM) (1 = probe, 2 = probe + $KO_2$, 3 = probe + $KO_2$ + GSH, 4 = probe + $KO_2$ + Cys, 5 = probe + $KO_2$ + Hcy, 6 = probe + $KO_2$ + NAC, 7 = probe + $KO_2$ + D-Meth) incubated for 2 min at rt, ($\lambda_{ex}$ = 573 nm, $\lambda_{em}$ = 608 nm), slit width 5/5 nm

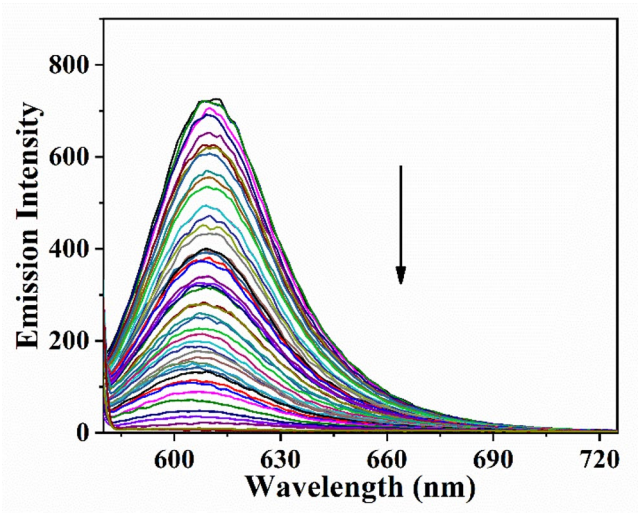


**Fig. 4** Emission spectra of probe **3** in DMSO with increasing concentration of $KO_2$ (0-800 µM) incubated for 2 min at rt ($\lambda_{ex}$ = 573 nm, $\lambda_{em}$ = 608 nm), slit width 5/5 nm

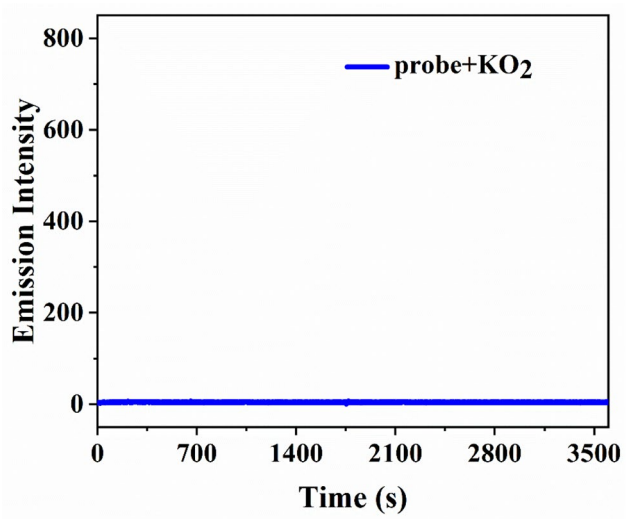


**Fig. 5** Time-dependent emission spectrum of probe **3** (5 µM) with $KO_2$ (800 µM) in DMSO at rt ($\lambda_{ex}$ = 573 nm, $\lambda_{em}$ = 608 nm), slit width 5/5 nm

Eq. 3σ/k and was found to be 4.87 µM for superoxide (Fig. S14).

For the time-dependent emission spectrum, $KO_2$ (24 µL, 800 µM) was added to probe **3** (3 mL, 5 µM) and spectrum was recorded in DMSO at rt (Fig. 5). Fluorescence of the probe with superoxide was quenched and found to be stable for longer time which confirmed the photostability with extremely quick response time for superoxide.

To study the fluorescence *turn-off* reaction mechanism, the reaction of probe **3** with $KO_2$ was carried out for 30 min in DMSO-$d_6$ (Scheme 2). The total consumption of the probe was monitored by TLC. Product (**4**) of the reaction was analyzed by $^1$H NMR spectroscopy and mass spectrometry (Figs. S10-11) without isolation. The $^1$H NMR spectrum of compound **4** showed a characteristic up-field shifts in proton signals as compared to probe **3** (Fig. S10). Molecular ion peak with selenium isotopic pattern was observed for compound **4** after subjecting to mass spectrometry with calculated mass for $(C_{45}H_{32}BF_2N_2SeO)^+$ of 743.5 $[M]^+$ and observed peak at m/z 743.5 for $[M]^+$ (Fig. S11). This confirmed the oxidation of selenium by superoxide.

The phenyl selenide group is unable to transport electrons to the BODIPY moiety once selenium is oxidized by superoxide, abolishing the Photoinduced Electron Transfer (PET), and the probe produces a fluorescence *turn-off* response. The PET mechanism has already been reported in depth in the literature [44, 45].

**Scheme 2** Synthesis of compound **4**

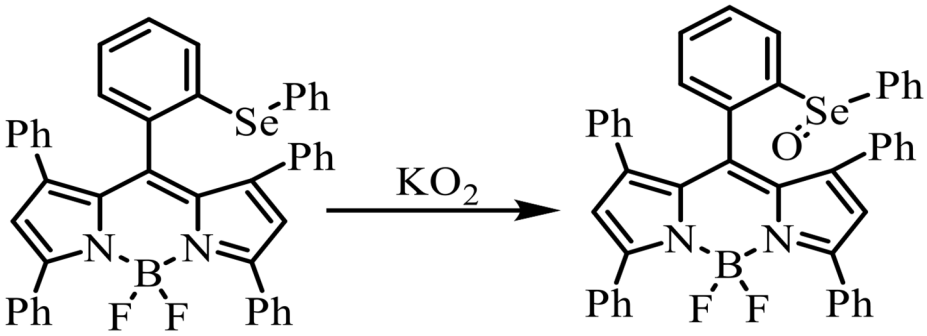


**3** **4**

## Conclusion

In conclusion, phenylselenyl-containing tetraphenyl substituted BODIPY-based probe was successfully synthesized and characterized using the spectroscopic and spectrometric techniques such as $^{1}$H, $^{13}$C, $^{77}$Se, $^{11}$B, $^{19}$F, and HR-LCMS. The tetraphenyl substituted Se-BODIPY-based probe was found to be selective and sensitive for the detection of superoxide over other ROS and biothiols. It has a *turn-off* (quenched) fluorescence response with detection limit of 4.87 µM. The probe with superoxide does not interfere with other ROS and biothiols. The probe reacted with superoxide rapidly in less than a sec with a stoke shift of 35 nm. The probe's high orange fluorescence is due to a Photoinduced Electron Transfer (PET) mechanism from the phenyl selenide group to the BODIPY core.

**Supplementary Information** The online version contains supplementary material available at https://doi.org/10.1007/s10895-022-03096-w.

**Acknowledgements** S. T. M. acknowledges the Science and Engineering Research Board (SERB), Govt. of India, New Delhi, for financial support (YSS/2014/000726). We acknowledge SAIF, IIT Bombay for core instrumentation facility. S. T. S acknowledges principal (Dr.) C. V. Murumkar, T. C. College Baramati, Maharashtra for their constant help and support.

**Author contribution** Shrikrishna T. Salunke: Designed, Methodology, Investigation, and characterization of compounds, spectrophotometric investigations, and preparation of manuscript. Divyesh S. Shelar: Methodology, Investigation, characterization of compounds, photophysical study, preparation of manuscript and formal analysis. Sudesh T. Manjare: Designed, characterization of compounds, supervision, writing, reviewing and editing.

**Funding** No funding was received for this study.

**Availability of data and material** Authors are declare that the data supporting the findings of this research are available within the article.

**Code Availability** Not applicable.

## Declarations

**Ethical Approval** Not applicable.

**Consent to Participate** Not applicable.

**Consent for publication** Not applicable.

**Competing Interests** The authors declare no competing interests.

## References

1. de Silva AP, Gunaratne HQN, Gunnlaugsson T et al (1997) Signaling recognition events with fluorescent sensors and switches. Chem Rev 97:1515–1566. https://doi.org/10.1021/cr960386p
2. Gunnlaugsson T, Glynn M, Tocci (née Hussey) GM, et al (2006) Anion recognition and sensing in organic and aqueous media using luminescent and colorimetric sensors. Coord Chem Rev 250:3094–3117. https://doi.org/10.1016/j.ccr.2006.08.017
3. Que EL, Domaille DW, Chang CJ (2008) Metals in Neurobiology: probing their Chemistry and Biology with Molecular Imaging. Chem Rev 108:1517–1549. https://doi.org/10.1021/cr800447y
4. Wang N, Wang H, Zhang J et al (2022) Endogenous peroxynitrite activated fluorescent probe for revealing anti-tuberculosis drug induced hepatotoxicity. Chin Chem Lett 33:1584–1588. https://doi.org/10.1016/j.cclet.2021.09.046
5. Yang X, Lu X, Wang J et al (2022) Near-Infrared fluorescent probe with a large Stokes Shift for detection of Hydrogen Sulfide in Food Spoilage, living cells, and zebrafish. J Agric Food Chem 70:3047–3055. https://doi.org/10.1021/acs.jafc.2c00087
6. Fan G, Wang N, Zhang J et al (2022) BODIPY-based near-infrared fluorescent probe for diagnosis drug-induced liver injury via imaging of HClO in cells and in vivo. Dyes Pigm 199:110073. https://doi.org/10.1016/j.dyepig.2021.110073
7. Chaudhury S, Sarkar PK (1983) Stimulation of tubulin synthesis by thyroid hormone in the developing rat brain. Biochim Biophys Acta - Mol Cell Res 763:93–98. https://doi.org/10.1016/0167-4889(83)90030-7
8. Kozumbo WJ, Trush MA, Kensler T (1985) Are free radicals involved in tumor promotion? Chem Biol Interact 54:199–207. https://doi.org/10.1016/S0009-2797(85)80163-0
9. Bulic B, Pickhardt M, Khlistunova I et al (2007) Rhodanine-based tau aggregation inhibitors in cell models of Tauopathy. Angew Chemie Int Ed 46:9215–9219. https://doi.org/10.1002/anie.200704051

10. Kepp KP (2012) Bioinorganic Chemistry of Alzheimer's Disease. Chem Rev 112:5193–5239. https://doi.org/10.1021/cr300009x
11. Gorman A, Killoran J, O'Shea C et al (2004) In Vitro demonstration of the heavy-atom effect for photodynamic therapy. J Am Chem Soc 126:10619–10631. https://doi.org/10.1021/ja047649e
12. Hattori S, Ohkubo K, Urano Y et al (2005) Charge separation in a nonfluorescent donor – acceptor Dyad Derived from Boron Dipyrromethene Dye, leading to Photocurrent Generation. J Phys Chem B 109:15368–15375. https://doi.org/10.1021/jp050952x
13. Qin W, Baruah M, Van Der Auweraer M et al (2005) Photophysical properties of borondipyrromethene analogues in solution. J Phys Chem A 109:7371–7384. https://doi.org/10.1021/jp052626n
14. Depauw A, Kumar N, Ha-Thi M-H, Leray I (2015) Calixarene-based fluorescent sensors for Cesium cations containing BODIPY fluorophore. J Phys Chem A 119:6065–6073. https://doi.org/10.1021/jp5120288
15. Boens N, Leen V, Dehaen W (2012) Fluorescent indicators based on BODIPY. Chem Soc Rev 41:1130–1172. https://doi.org/10.1039/C1CS15132K
16. Shahrokhian S (2001) Lead phthalocyanine as a selective carrier for Preparation of a cysteine-selective electrode. Anal Chem 73:5972–5978. https://doi.org/10.1021/ac010541m
17. Vu TT, Badré S, Dumas-Verdes C et al (2009) New Hindered BODIPY derivatives: solution and amorphous state fluorescence Properties. J Phys Chem C 113:11844–11855. https://doi.org/10.1021/jp9019602
18. Manjare ST, Kim Y, Churchill DG (2014) Selenium- and Tellurium-Containing fluorescent Molecular Probes for the detection of biologically important Analytes. Acc Chem Res 47:2985–2998. https://doi.org/10.1021/ar500187v
19. Lou Z, Li P, Han K (2015) Redox-responsive fluorescent probes with different design strategies. Acc Chem Res 48:1358–1368. https://doi.org/10.1021/acs.accounts.5b00009
20. Nogueira CW, Zeni G, Rocha JBT (2004) Organoselenium and Organotellurium Compounds: Toxicology and Pharmacology. Chem Rev 104:6255–6285. https://doi.org/10.1021/cr0406559
21. Mukherjee AJ, Zade SS, Singh HB, Sunoj RB (2010) Organoselenium Chemistry: role of intramolecular interactions. Chem Rev 110:4357–4416. https://doi.org/10.1021/cr900352j
22. Mugesh G, du Mont W-W, Sies H (2001) Chemistry of biologically important synthetic organoselenium compounds. Chem Rev 101:2125–2179. https://doi.org/10.1021/cr000426w
23. Shelar DS, Dhavan PP, Singh PR et al (2021) Synthesis and study of organoselenium compound: DNA/Protein interactions, in vitro antibacterial, antioxidant, anti-inflammatory activities and anticancer activity against carcinoma cells. J Mol Struct 1244:130914. https://doi.org/10.1016/j.molstruc.2021.130914
24. Poirel A, De Nicola A, Ziessel R (2012) Oligothienyl-BODIPYs: Red and Near-Infrared Emitters. Org Lett 14:5696–5699. https://doi.org/10.1021/ol302710z
25. Sedgwick AC, Wu L, Han H-H et al (2018) Excited-state intramolecular proton-transfer (ESIPT) based fluorescence sensors and imaging agents. Chem Soc Rev 47:8842–8880. https://doi.org/10.1039/C8CS00185E
26. Wu D, Chen L, Kwon N, Yoon J (2016) Fluorescent probes containing selenium as a guest or host. Chem 1:674–698. https://doi.org/10.1016/j.chempr.2016.10.005
27. Balkrishna SJ, Hodage AS, Kumar S et al (2014) Sensitive and regenerable organochalcogen probes for the colorimetric detection of thiols. RSC Adv 4:11535–11538. https://doi.org/10.1039/C4RA00381K
28. Loudet A, Burgess K (2007) BODIPY dyes and their derivatives: Syntheses and Spectroscopic Properties. Chem Rev 107:4891–4932. https://doi.org/10.1021/cr078381n
29. Yang J, Liu X, Wang H et al (2018) A turn-on near-infrared fluorescence probe with aggregation-induced emission based on dibenzo[ a, c ]phenazine for detection of superoxide anions and its application in cell imaging. Analyst 143:1242–1249. https://doi.org/10.1039/C7AN01860F
30. Venkatesan P, Wu S-P (2015) A turn-on fluorescent probe for hypochlorous acid based on the oxidation of diphenyl telluride. Analyst 140:1349–1355. https://doi.org/10.1039/C4AN02116A
31. Zhang W, Liu W, Li P et al (2015) Reversible two-photon fluorescent probe for imaging of hypochlorous acid in live cells and in vivo. Chem Commun 51:10150–10153. https://doi.org/10.1039/C5CC02537K
32. Mulay SV, Choi M, Jang YJ et al (2016) Enhanced fluorescence turn-on imaging of Hypochlorous Acid in living Immune and Cancer cells. Chem - A Eur J 22:9642–9648. https://doi.org/10.1002/chem.201601270
33. Panda S, Panda A, Zade SS (2015) Organoselenium compounds as fluorescent probes. Coord Chem Rev 300:86–100. https://doi.org/10.1016/j.ccr.2015.04.006
34. Mulay SV, Yudhistira T, Choi M et al (2016) Substituent Effects in BODIPY in Live Cell Imaging. Chem - An Asian J 11:3598–3605. https://doi.org/10.1002/asia.201601400
35. Deshmukh PP, Navalkar A, Maji SK, Manjare ST (2019) Phenylselenyl containing turn-on dibodipy probe for selective detection of superoxide in mammalian breast cancer cell line. Sens Actuators B Chem 281:8–13. https://doi.org/10.1016/j.snb.2018.10.072
36. Madibone KS, Deshmukh PP, Navalkar A et al (2020) Cyclic Organoselenide BODIPY-Based probe: Targeting Superoxide in MCF – 7 Cancer cells. ACS Omega 5:14186–14193. https://doi.org/10.1021/acsomega.0c02074
37. Malankar GS, Sakunthala A, Navalkar A et al (2021) Organoselenium-based BOPHY as a sensor for detection of hypochlorous acid in mammalian cells. Anal Chim Acta 1150:338205. https://doi.org/10.1016/j.aca.2021.338205
38. Shelar DS, Malankar GS, Manikandan M et al (2022) Selective detection of hypochlorous acid in living cervical cancer cells with an organoselenium-based BOPPY probe. New J Chem 46:17610–17618. https://doi.org/10.1039/D2NJ02956A
39. Dubey R, Lee H, Nam D-H, Lim D (2011) Mild generation of selenolate nucleophiles by thiol reduction of diselenides: convenient syntheses of selenyl-substituted aryl aldehydes. Tetrahedron Lett 52:6839–6842. https://doi.org/10.1016/j.tetlet.2011.10.075
40. Adib M, Ayashi N, Heidari F, Mirzaei P (2016) Reaction between 4-Nitro-1,3-diarylbutan-1-ones and ammonium acetate in the Presence of Morpholine and Sulfur: an efficient synthesis of 2,4-Diarylpyrroles. Synlett 27:1738–1742. https://doi.org/10.1055/s-0035-1561852
41. Manjare ST, Kim S, Heo W, Do, Churchill DG (2014) Selective and sensitive superoxide detection with a New Diselenide -Based molecular probe in living breast Cancer cells. Org Lett 16:410–412. https://doi.org/10.1021/ol4033013
42. Ahmed MG, Romman U, Ahmed SM et al (2007) Synthesis and correlation of Spectral Properties of some substituted 1,3-Diphenyl-2-Propen-1-Ones. Bangladesh J Sci Ind Res 42:45–52. https://doi.org/10.3329/bjsir.v42i1.354
43. Zhang G, Zhu C, Liu D et al (2017) Solvent-free enantioselective conjugate addition and bioactivities of nitromethane to Chalcone containing pyridine. Tetrahedron 73:129–136. https://doi.org/10.1016/j.tet.2016.11.063
44. Liu S-R, Wu S-P (2013) Hypochlorous Acid turn-on fluorescent probe based on oxidation of Diphenyl Selenide. Org Lett 15:878–881. https://doi.org/10.1021/ol400011u
45. Lou Z, Li P, Pan Q, Han K (2013) A reversible fluorescent probe for detecting hypochloric acid in living cells and animals: utilizing a novel strategy for effectively modulating the fluorescence of selenide and selenoxide. Chem Commun 49:2445–2447. https://doi.org/10.1039/c3cc39269d